Title: Remote sensing monitoring and evaluation of the temporal and spatial changes in the eco-environment of a typical arid land of the Tarim Basin in Western China

Author: Lingxiao Sun, Yang Yu, Yuting Gao, Ireneusz Malik, Malgorzata Wistuba, Ruide Yu [i in.]

UNIWERSYTET ŚLĄSKI
W KATOWICACH

Biblioteka
Uniwersytetu Śląskiego

Ministerstwo Nauki
i Szkolnictwa Wyższego

Remote Sensing Monitoring and Evaluation of the Temporal and Spatial Changes in the Eco-Environment of a Typical Arid Land of the Tarim Basin in Western China

Lingxiao Sun [1,2,3] iD, **Yang Yu** [1,2,3,4,*], **Yuting Gao** [1,2,3], **Jing He** [1,2,3], **Xiang Yu** [1,3], **Ireneusz Malik** [1,4], **Malgorzata Wistuba** [1,4] iD and **Ruide Yu** [1,3,4,5]

1   State Key Laboratory of Desert and Oasis Ecology, Xinjiang Institute of Ecology and Geography, Chinese Academy of Sciences, Urumqi 830011, China; sunlingxiao18@mails.ucas.ac.cn (L.S.); gaoyuting18@mails.ucas.ac.cn (Y.G.); hejing20@mails.ucas.ac.cn (J.H.); yuxiang21@mails.ucas.ac.cn (X.Y.); irekgeo@wp.pl (I.M.); malgorzata.wistuba@us.edu.pl (M.W.); ruideyu@ms.xjb.ac.cn (R.Y.)
2   Cele National Station of Observation and Research for Desert-Grassland Ecosystems, Cele 848300, China
3   Chinese Academy of Sciences, Beijing 100049, China
4   Polish-Chinese Centre for Environmental Research, Institute of Earth Sciences, University of Silesia in Katowice, 60 Będzińska, 41-200 Sosnowiec, Poland
5   School of Environment and Material Engineering, Yantai University, Yantai 264005, China
*   Correspondence: yuyang@ms.xjb.ac.cn

Abstract: The eco-environment provides various spaces, conditions, and resources for human development, and their quality is a significant factor affecting sustainable development in a region. Most drylands face environmental fragility due to problems such as infertile land, scarce suitable living space, and a lack of resources. Therefore, investigating the temporal and spatial changes in the eco-environment of drylands is vital to developing them sustainably. This paper takes Hetian, which is located in the Tarim Basin of Western China and has typical features of an arid (or a hyper-arid) region, as the research area. The ecological index (EI) was used to construct a comprehensive ecological evaluation system, and five sub-indices (the biological richness index, vegetation coverage index, water network denseness index, land stress index, and pollution load index) were calculated to identify the quality and changes in the eco-environment of Hetian in 1995, 2009, and 2018. The results show that, from 1995 to 2018, the EI in Hetian showed a continuous downward trend (from 24.76 to 16.32), representing a change (ΔEI) of −8.44; this indicates significant deterioration in the quality of the local eco-environment. Large fluctuations in the EI also suggests that the environment in Hetian is very sensitive. In addition, the results revealed a degradation of Hetian, which includes a hyper-arid region.

Keywords: eco-environment; ecological index; biological richness; vegetation coverage; water network denseness; land stress; pollution load; desertification; arid land

1. Introduction

The eco-environment can be defined as the total of various natural forces or their effects closely related to humankind, and it plays a vital role to human development because it provides people with living spaces and various resources [1–3]. With rapid development, people's demand for resources and dependence on the natural environment have increased in recent decades [4,5]. In the process, people have inevitably caused damage to the environment, which has led to many environmental problems such as global warming, extreme weather, pollution, water shortages, land degradation, soil erosion, and forest reduction [6–9]. Frequent environmental issues pose a threat to the development of human society and economy [10–13]; therefore, observing, analyzing, and evaluating the eco-environment in a region through scientific methods allow for monitoring

local environmental changes directly, allowing potential environmental problems to be discovered and solved in time.

To analyze the eco-environment more thoroughly, some people have integrated various indicators to form a comprehensive one through mathematical methods to evaluate the overall environmental quality of a region. For instance, the multi-level fuzzy comprehensive evaluation method was applied to evaluate urban environmental quality in early research, which combines fuzzy clustering with step analysis [14]. The step analysis method is also an effective way to assess urban environmental quality, and it is based on a principle that divides influence factors into different categories. After analyzing each category step by step, the local environmental quality can be acquired [15]. The grey evaluation model is used to identify the regional environmental quality by determining the weight coefficients in each index category and by superimposing the weight coefficients of the same category of each evaluation index to obtain a comprehensive weight coefficient matrix of the evaluation object. Based on this, a triangular coordinate diagram can be used to comprehensively analyze and classify evaluation objects, thus avoiding the problems with the commonly used index method [16]. In addition, the artificial neural network is also a feasible approach to investigate eco-environment problems. Back-propagation (BP) is a widely used neural network trained by the error backward propagation algorithm. A trained BP network was used to analyze environmental quality, and its results were compared with those from a fuzzy recognition evaluation method. The evaluation results from the artificial neural network were consistent with the actual environmental quality [17]. These methods were widely adopted in environmental quality monitoring from 2000 to 2010, but the evaluation system established using these methods contains numerous indicators that usually require a large amount of data to support, which makes the evaluation difficult.

The comprehensive index method has been widely used to evaluate the eco-environment recently. It converts factors that affect the environment into individual indices of the same scale, which is convenient for integrating different factors, and it can be used as the basis for ranking the eco-environment quality in different regions. The weight of each index is determined according to its importance. The principle of the comprehensive index method is to multiply the weights calculated by the analytic hierarchy process (AHP) and the values obtained by the fuzzy evaluation method, then add them together, and finally calculate the total eco-environment value to reflect the environmental quality [18]. There are two common comprehensive indexes: the remote sensing ecological index (RSEI) and the ecological index (EI). The RSEI is based on remote sensing images and extracts four ecological indicators—greenness, humidity, dryness, and heat—to globally reflect the regional eco-environment and realize the aggregation of multi-dimensional indicators through principal component transformation [19,20]. The advantage of the RSEI is that it overcomes the shortcomings of single index methods by only selecting a few essential variables. It is currently the most widely used evaluation method for the eco-environment. The *Technical Criterion for Ecosystem Status Evaluation (HJ192-2015)*, issued in 2005 by China's Ministry of Ecology and Environment, reformulated the standards for a comprehensive evaluation, using the ecological index (EI) to reflect the overall status of a regional eco-environment [21]. Compared with RSEI, the evaluation system constructed using EI is more comprehensive, including five indicators: biological richness, vegetation coverage, water network denseness, land stress, and pollution load.

EI has broad applicability, many scholars have used it for eco-environmental evaluation in recent years. For example, Zhang (2012) used EI to identify the change in eco-environmental quality of the Tekes watershed from 1990 to 2010. The results showed that the eco-environment of the Tekes watershed had improved from 2000 to 2010, after a trend of degradation from 1990 to 2000. These results match with the observed data [22]. Lin (2019) adopted EI to evaluate the eco-environmental quality in the Danjiangkou Reservoir, and the ecosystem service value index was added to assess the eco-environment from an economic point of view [23]. Gong and Li (2020) addressed EI to analyze the natural

and ecological conditions of the Tibet Plateau ecological shelter zone in 2017 and 2018. The results indicated that the EI had not changed markedly from 2017 to 2018 [24]. The natural environment is diverse in China, and despite using EI only within one country, it has been implemented in different ecotones. In short, EI is more suitable for evaluating the eco-environmental quality at a large spatial and temporal scale. Landsat, MODIS, and Sentinel are good data sources because their products are easily accessible, and it is easier to calculate the sub-indices of EI with moderate-resolution imagery. Another advantage of EI is that the calculation is simple and feasible, reflecting the comprehensiveness and integrity of the eco-environment. Furthermore, the eco-environment quality level of each region is clearly defined and sorted so that the evaluation results are clear and easy to compare [25,26]. However, the shortcoming of EI is that it has a high demand for statistical data such as hydrological, meteorological, and pollution load data, and collecting these data requires a sufficient budget and time. In addition, the weight allocation of each sub-index of EI is relatively subjective, and it may not be appropriate for regions with a different landscape and climate [27,28]. Therefore, for different regions, the chosen sub-indices and the allocation of weights need to be adjusted according to local conditions.

The Hetian area, located in the Tarim Basin of Xinjiang, Western China, is a deep interior land located far away from the ocean. The climate is extremely dry throughout the year, water resources are scarce, sandstorms are frequent, desertification is severe, and the ecosystem is highly fragile [29]. Therefore, monitoring its eco-environment is of great significance for local sustainable development. The goal of this study was to identify the quality of the eco-environment in Hetian in 1995, 2009, and 2018 through a comprehensive index method—EI. To achieve this goal, we set the following three research objectives: (i) to calculate five sub-indices and the total value of EI in each studied year, (ii) to analyze the changes in the eco-environmental status in the past 25 years, and (iii) to discuss the possible causes and effects for those changes and reveal policies implication.

2. Materials and Methods

2.1. Overview of the Research Area

In this paper, the research area refers to the Hetian area, located in the Tarim Basin of Xinjiang, Western China, centered at 79.92° E longitude and 37.12° N latitude. Hetian has jurisdiction over a county-level city and seven counties in total (Figure 1). The topography of the research area is low in the north and high in the south, with basins and oases in the north and mountainous highlands in the south. Hetian includes the Taklamakan Desert, one of the driest deserts in the world. Most lands of Hetian are arid and hyper-arid areas. The aridity index can reflect the degree of drought in a region. In most parts of Hetian, the aridity index is consistently under 0.1, which indicates the severe aridity condition [30]. The main feature of arid and hyper-arid areas is scarce precipitation throughout the year. The average annual rainfall in Hetian is 35 mm, and the annual evaporation is 2480 mm. The sand-dust weather occurs frequently in every season in Hetian, which accounts for more than 220 days each year, of which sandstorm weather accounts for ~60 days. The total land area of Hetian is 24.93 million hectares, of which the mountainous area accounts for 44.5% and the plain area accounts for 55.5%. The mountainous regions consist of 42% bare rock and gravel that are difficult to develop (although there are some grasslands, glaciers, and a small amount of arable and forested land). More than 90% of the plains are desert, while oases, which cover 9730 square kilometers, account for only 3.96% of the total land area. The annual average surface water runoff in Hetian is 7335 million cubic meters. The glaciers in the high mountainous region in the south are the source of inland rivers in the south of the Tarim Basin and are important supply sources for the main rivers in Hetian. At the end of 2018, the total registered population of the entire area was 2.53 million; the urban population was 548,600, and the rural population was 1.98 million. In 2018, the whole region achieved a gross domestic product (GDP) of CNY 30.56 billion and a per capita GDP of CNY 12,094, which reached a peak value compared to the past few decades [31,32].
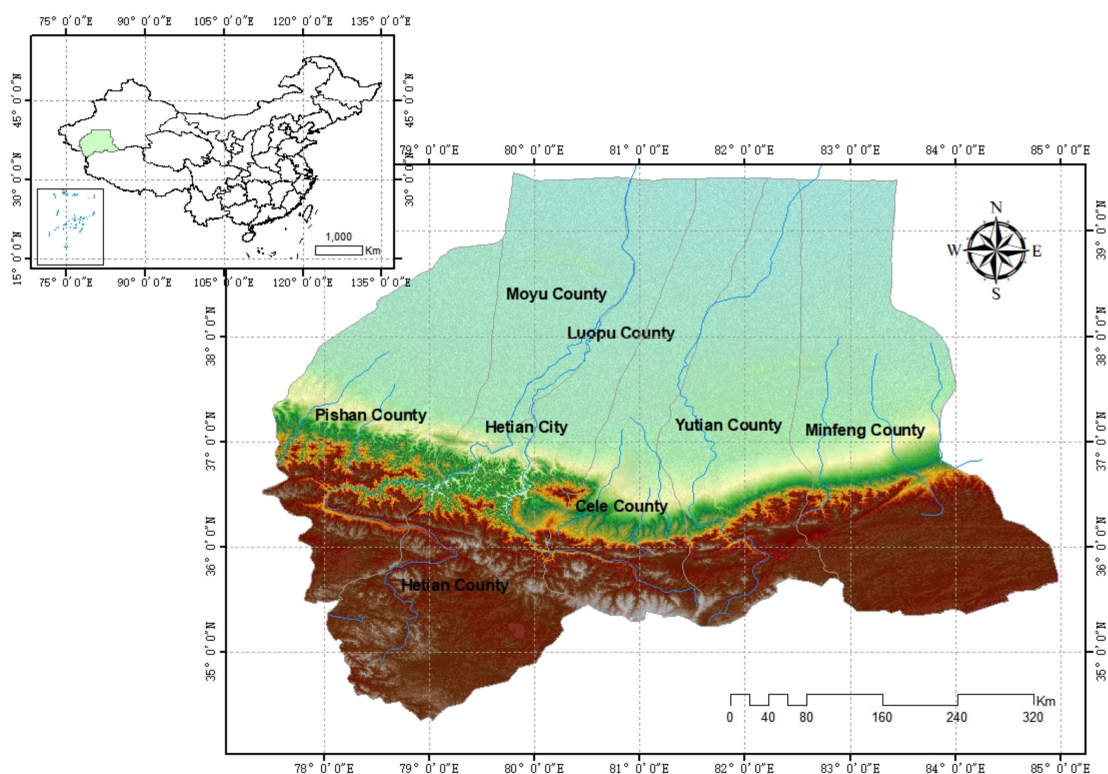
Figure 1. Geographical overview of Hetian.

In general, Hetian is in an extremely dry environment, and its ecosystem is very fragile. The oases are prone to desertification, leading to a change in the oasis environment and the overall deterioration of the eco-environment. According to the definition of the United Nation Convention to Combat Desertification, this problem is defined as "land degradation in arid, semi-arid and dry subhumid areas resulting from various factors, including climatic variations and human activities". Land degradation refers to the reduction in or loss of the biological or economic productivity of the land, which includes soil erosion, soil salinization, groundwater degradation, or sandification processes [33]. The causes of land desertification include climate variations, such as droughts, and excessive human activities, such as overgrazing, deforestation, land reclamation, and unreasonable use of water resources. Desertification leads to a reduction in available land resources, the decline of land productivity, and the aggravation of natural disasters [34,35]. Therefore, exploring the temporal and spatial evolution processes and current situation of the local eco-environment is of great significance for future sustainability and also assessing the desertification of Hetian.

2.2. Research Data and Sources

2.2.1. Landsat Remote Sensing Image Data

The remote sensing data used in this research are a digital product from the Landsat remote sensing image data service system established by the Computer Network Information Center of the Chinese Academy of Sciences (http://ids.ceode.ac.cn/ (accessed on 10 October 2020)). The data were mirrored from the US Landsat series images taken by the United States Geological Survey, and the time span was from 1995 to 2018. The data for 1995 were from the Landsat 5 TM satellite digital product, with a spatial resolution of 30 m; those for 2009 were from the Landsat 7 ETM SLC-on product, with a spatial resolution of 30 m, and those for 2018 were from the Landsat 8 OLI_TIRS satellite digital product, with a spatial resolution of 15 m. To make sure the images cover the entire Hetian area, the data in each phase included 15 scene images, which were spliced into a complete remote sensing

image of the research area using mosaicking technology. The imaging time was from May to September, and the cloud content was <10%. The data format was GeoTIFF (including header files) from a Level-1 Product Generation System (LPGS). The Landsat images were used for land use classification, and then for calculation of the biological richness index, water network denseness index, and land stress index.

2.2.2. MODIS Sensor Data

The vegetation coverage index was calculated using NDVI data from the MODIS sensor's MOD13 series products from May to September for all of the years. MOD13 refers to the Version 6 data obtained by the MODIS sensor mounted on the Terra satellite. The data are generated once every 16 days with a spatial resolution of 250 m; it is a Level 3 product. The data were sourced from the Geospatial Data Cloud (http://www.gscloud.cn (accessed on 16 February 2021)) and the NASA Earthdata Search (https://search.earthdata.nasa.gov/ (accessed on 16 February 2021)).

2.2.3. DEM Data

The DEM data were obtained from the Shuttle Radar Topography Mission topographical product data jointly released by NASA and NIMA with a 90-m spatial resolution. The data download address is the Geospatial Data Cloud (http://www.gscloud.cn (accessed on 2 February 2021)).

2.2.4. Hydrological Data

The hydrological data used in this research include the surface water resources, underground water resources, and total water resources in Hetian. The data were obtained from the Xinjiang Statistical Yearbook of the Xinjiang Uygur Autonomous Region Statistics Department for all years.

2.2.5. Meteorological Data

The meteorological data in this research comprise the total annual precipitation data for the Hetian area in 1995, 2009, and 2018. The data were obtained from the Hetian Yearbook issued by the Hetian Statistics Bureau.

2.2.6. Pollution Data

The data used to calculate the pollution load index included the emissions of chemical oxygen demand (COD), ammonia nitrogen, sulfur dioxide, smoke and dust, nitrogen oxides, and solid waste. These data were obtained from the "Statistics of Urban Life Pollution Emissions and Treatments" in the Hetian Yearbook for all studied periods.

2.3. Construction of the Ecological Index

Following the *Technical Criterion for Ecosystem Status Evaluation (HJ192-2015)*, issued in 2015 by the Ministry of Ecology and Environment of the People's Republic of China, this study constructed a comprehensive index—the EI—to evaluate the eco-environment status and used the remote sensing information of Hetian to identify the eco-environmental quality and its temporal and spatial changes. The EI includes five sub-indices, and they are biological richness index, vegetation coverage index, water network denseness index, land stress index, and pollution load index. The EI was calculated as follows [21]:

$$
\begin{aligned}
EI = \sum_{i=1}^{n} K_i B_i = {}& 0.35 * \text{Biological Richness Index} \\
& + 0.25 * \text{Vegetation Coverage Index} \\
& + 0.15 * \text{Water Network Denseness Index} \\
& + 0.15 * (100 - \text{Land Stress Index}) \\
& + 0.10 * \text{Pollution Load}
\end{aligned}
\tag{1}
$$

where B_i represents the sub-indices of the eco-environmental evaluation, K_i represents the weights of these indices, and n is the number of indices participating in the evaluation

of the eco-environmental quality. These weighting factors were referenced from *Technical Criterion for Ecosystem Status Evaluation (HJ192-2015)*, weighting factors were calculated by the AHP. To construct an EI, experts should build a hierarchical model by analyzing what kind of factors may influence the quality of eco-environment firstly. Then the related factors were stratified according to its attributes and importance. After the calculation of comparison-matrix and the weight vector, the weight of each factor can be determined. The range value for each sub-index was set at 0 to 100. Any individual values for a sub-index outside this range would be assigned the respective minima or maxima.

2.3.1. Biological Richness Index

The biological richness index is an indicator used to evaluate the abundance and deficiency of organisms and habitats in a research area [36–38]. According to *Technical Criterion for Ecosystem Status Evaluation (HJ192-2015)*, the biological richness index is determined by the biodiversity and the quality of habitats. When the biodiversity index has no dynamically updated data, the biological richness index can be represented by the habitat quality index. Since no data show that the biodiversity of Hetian has significantly changed in recent years, this paper used only the habitat quality index to evaluate the local biological abundance. A habitat can be defined as "A place where an organism or a community of organisms lives, including all living and nonliving factors or conditions of the surrounding environment" [39]. The functions of a habitat are providing resources and conditions for the survival and reproduction of species [40,41]. The habitat quality of an area can be assessed by evaluating the land use/cover change (LUCC) in this area. Based on the standards of the *Land Use Status Classification (GBT 21010-2017)* issued by the Ministry of Land and Resources of China, this paper established six first-level land use types: forest, grassland, water surfaces, agriculture, urban or built-up, and barren land. The calculation formula for the habitat quality index can be expressed as follows:

$$\text{Habitat Quality Index} = \frac{A_{bio} \times (0.35 \times \text{Forest} + 0.21 \times \text{Grassland} + 0.28 \times \text{Water Surfaces} + 0.11 \times \text{Agriculture} + 0.04 \times \text{Urban or Built-up} + 0.01 \times \text{Barren Land})}{\text{Total Area}} \quad (2)$$

where A_{bio} is the normalization coefficient of the habitat quality index, and the reference value is 511.26. In this paper, the function of normalization coefficients is to make the calculated results of each index between 0 and 100, which helps results easy to be compared and evaluated. The calculation method of each normalization coefficient is shown as below:

$$\text{Normalization Coefficient} = 100/A_{Max} \quad (3)$$

where A_{Max} is the maximum value of the exponent before normalization. In addition, the results of land use classification will be validated by accuracy assessment, which is a quantitative analysis in which the accuracy of the results is verified by an error matrix. The same data source is used to classify the field sampling points according to the same classification method, and then the results of the two classifications are compared.

2.3.2. Vegetation Coverage Index

The vegetation coverage index indicates the amount of vegetation cover, which is essential for the protection of eco-environment, especially in drylands. Since the MODIS sensor's MOD13-series products provide directly usable NDVI data, this research employed the Band Math function of the ENVI software to calculate the average monthly maximum value of the NDVI data from May to September in the studied period [21]. The calculation formula is as follows:

$$\text{Vegetation Coverage Index} = \text{NDVI}_{\text{Regional Averages}} = A_{veg} * \left(\frac{\sum_{i=1}^{n} P_i}{n} \right) \quad (4)$$

where P_i is the average monthly maximum value of NDVI from May to September; n is the number of regional pixels; and A_{veg} is the normalization coefficient of the vegetation coverage index, for which the reference value is 0.01.

After the results were obtained, they were divided into five categories according to the vegetation coverage, as shown in Table 1.

Table 1. Classification of vegetation coverage.

Level	Categories	Vegetation Coverage Rate (%)	Descriptions
I	Extremely Low	0~20%	Vegetation coverage rate is extremely low; only has little vegetation; almost barren lands.
II	Low	20~40%	Vegetation coverage rate is low; has little vegetation.
III	Medium	40~60%	Vegetation coverage rate is medium; has some vegetation, but not dense.
IV	High	60~80%	Vegetation coverage rate is high; has much vegetation.
V	Extremely High	80~100%	Vegetation coverage rate is extremely high; has a great amount of vegetation; vegetation cover is dense.

2.3.3. Water Network Denseness Index

The water network denseness index is an indicator used to evaluate the abundance of water resources in a region. It refers to the proportion of the total length of rivers, lakes, and water resources in the evaluated area and reflects the abundance of water. The calculation formula is as follows:

$$\text{Water Network Denseness Index} = \frac{1}{3} \times \frac{A_{riv} \times \text{River Length}}{\text{Total Area}} + \frac{1}{3} \times \frac{A_{lak} \times \text{Lake Arae}}{\text{Total Area}} + \frac{1}{3} \times \frac{A_{res} \times \text{Water Resourses Volume}}{\text{Total Area}} \quad (5)$$

where A_{riv} is the normalization coefficient of river length, for which the reference value is 84.37; A_{lak} is the normalization coefficient of the lake area, and its reference value is 591.79; and A_{res} is the normalization coefficient of water resources' quantity, for which the reference value is 86.39.

First, the calculation of river length relied on the spatial analysis tools of ArcGIS software. Using six analytical procedures—namely fill, flow direction, flow accumulation, raster calculator, stream order, and stream to feature—on the DEM data in Hetian, the water basin system could be effectively extracted to calculate the river length. It should be emphasized that rivers in an arid or hyper-arid area contain ephemeral and permanent parts. During the rainy season, rainwater flows into rivers; while in the dry season, the flow becomes smaller and even dries up, leaving only the riverbed. In this study, we set a threshold for the flow accumulation, and when the flow of a river was greater than this value, the river was counted into the total length. Images this study used came from the rainy season (June~August), so the calculation included both ephemeral and permanent streams. Second, to calculate the total areas of lakes included in Hetian, the slope tool of ArcGIS was used. The principle is based on Earth's gravity and the formation principle of large water bodies. The surface slope of large water bodies is tiny; therefore, after slope analysis of topographic data, pixels with zero slope were retained and focus statistics were performed to extract the research area's water system. Then, the raster data were vectorized to calculate the area of the local lakes, and finally, the water resource volume was directly extracted from the statistical yearbook of Hetian.

2.3.4. Calculation of Land Stress Index

The land stress index is used to identify the degree to which the land quality in an evaluation area is under stress. The degree of land stress is related to the degree of soil erosion. As Hetian is located in the Tarim Basin—which has sparse vegetation, a dry climate, deficient annual precipitation, frequent strong winds and sandstorms, and many mobile and semi-mobile dunes—the erosion agent is wind, but erosion is triggered by the

loss of vegetal cover, which is related to land use changes. The Standards for *Classification and Gradation of Soil Erosion (SL190-2007)* issued by the Ministry of Water Resources of China were used in this research as a basis for formulating the classification and grading standards for the soil erosion degree in Hetian. The soil erosion level was divided into five categories from weak to strong according to its degree, namely I slight, II mild, III moderate, IV strong, and V severe (Table 2).

Table 2. Classification and grading standards of soil erosion in Hetian.

Level	Vegetation Coverage Rate (%)	Slope (°)	Land Use Types
I Slight	>70	0–8	Water Surfaces
II Mild	70–50	8–15	Forest
III Moderate	50–30	15–25	Agriculture
IV Strong	30–10	25–35	Grassland
V Severe	<10	>35	Barren Land

ArcGIS was used to analyze the factors that affect soil erosion (vegetation coverage, slope, and land use types) and then to conduct a spatial overlay analysis and reclassify the results to obtain an overview of the soil erosion distribution in Hetian. After that, the land stress index was calculated according to the following formula:

$$\text{Land Stress Index} = \frac{A_{ero} \times (0.4 \times \text{Severe Erosion Area} + 0.2 \times \text{Strong Erosion Area} + 0.2 \times \text{Urban or Build-up Area} + 0.2 \times \text{Other Erosion Area})}{\text{Total Area}} \tag{6}$$

where A_{ero} is the normalization coefficient of the land stress index, for which the reference value is 236.04.

2.3.5. Calculation of Pollution Load Index

The pollution load index can be used to evaluate the degree of pollution in an area. It is an evaluation method proposed by Tomlinson and colleagues in a classification study of the heavy metal pollution level and is mainly aimed at assessing the contributions of different forms of pollution and the changes in time and space [42]. The calculation formula is presented as follows:

$$\text{Pullution Load Index} = \frac{0.2 \times A_{COD} \times COD_{Emissions}}{\text{Annual Precipitation}} + \frac{0.2 \times A_{NH3} \times \text{Ammoina Nitrogen Emissions}}{\text{Annual Precipitation}} + \frac{0.2 \times A_{so_2} \times SO_{2 Emissions}}{\text{Total Area}} + \frac{0.1 \times A_{YFC} \times \text{Smoke and Dust Emissions}}{\text{Total Area}} + \frac{0.2 \times A_{NOX} \times \text{Nitrogen Oxides Emissions}}{\text{Total Area}} + \frac{0.1 \times A_{SOL} \times \text{Soil Waster Emissions}}{\text{Total Area}} \tag{7}$$

where A_{COD} is the normalization index of chemical oxygen demand, whose reference value is 4.39; A_{NH3} is the normalization index of ammonia nitrogen, for which the reference value is 40.18; A_{SO2} is the normalization index of sulfur dioxide, and its reference value is 0.06; A_{YFC} is the normalization index of smoke and dust, for which the reference value is 4.09; A_{NOX} is the normalization index of nitrogen oxide, whose reference value is 0.51; and A_{SOL} is the normalization index of solid waste, for which the reference value is 0.07.

2.3.6. Classification and Analysis of Change in Eco-Environmental Status

According to the EI calculation result, the eco-environmental status was divided into five levels, namely excellent, good, moderate, relatively poor, and poor. The grading standards are shown in Table 3.

Table 3. Grading standards of the eco-environmental status.

Level	The Value of EI	Descriptions
Excellent	EI ≥ 75	High vegetation coverage; abundant biodiversity; stable ecosystem; extremely livable.
Good	55 ≤ EI < 75	Good vegetation coverage and biodiversity; livable.
Moderate	35 ≤ EI < 55	Moderate vegetation coverage and biodiversity; relatively livable; a few restrictive factors for people's living.
Relatively poor	20 ≤ EI < 35	Relatively poor vegetation coverage and biodiversity; not livable; some restrictive factors for people's living.
Poor	EI < 20	Poor vegetation coverage and biodiversity; not livable; many restrictive factors for people's living.

According to the changes in EI and the benchmark value, the eco-environmental change range was divided into four levels: no obvious change, slight change, obvious change, and significant change. The change values and evaluation methods of all levels are shown in Table 4.

Table 4. Grading of the change degree of the eco-environmental status.

Level	Variation	Descriptions
No obvious change	$|\Delta EI| < 1$	The eco-environment quality has no obvious change.
Slight change	$1 \leq |\Delta EI| < 3$	If $1 \leq \Delta EI < 3$, the eco-environment quality has improved slightly; if $-1 \geq \Delta EI > -3$, it has deteriorated slightly.
Obvious change	$3 \leq |\Delta EI| < 8$	If $3 \leq \Delta EI < 8$, the eco-environment quality has improved obviously; if $-3 \geq \Delta EI > -8$, it has deteriorated obviously.
Significant change	$|\Delta EI| \geq 8$	If $\Delta EI \geq 8$, the eco-environment quality has improved significantly; if $\Delta EI \leq -8$, it has deteriorated significantly.

3. Results

3.1. Biological Richness Index

Table 5 and Figure 2 show that between 1995 and 2018, the forest area in Hetian declined significantly, where it decreased from 33,639.13 km² to 16,877.6 km² (nearly 7%). The area of grassland increased sharply between 1995 and 2009, after which it decreased 4.15% between 2009 and 2018, but the overall area increased from 1995 to 2018. For water surfaces, its area expanded 0.69-fold between 1995 and 2009. Then it reduced slightly between 2009 and 2018. The overall area of water surfaces increased from 13,585.53 km² to 21,798.6 km² between 1995 and 2018. The areas of agriculture and urban or built-up also increased from 1995 to 2018, with the agriculture area increasing by 2.23%. The growth of urban or built-up is even more significant, from 0.99% to 9.15%, representing an increase by 8.16%. Although barren land had always accounted for the largest proportion, with the increase in grassland, water surfaces, agriculture, and urban or built-up, the area of barren land decreased continuously from 1995 to 2018. As of 2018, the barren land area was 157,339 km², accounting for 63.82% of the total area—11.47% less than in 1995.

3.2. Vegetation Coverage Index

According to Table 6 and Figure 3, in the three years of 2000, 2009, and 2018, low and extremely low coverage land areas in Hetian accounted for ~89% of the total area on average, meaning that vegetation was scarce in most areas in Hetian, the vegetation coverage rate was extremely low, and there was much bare land. Areas with moderate, high, and extremely high vegetation coverage showed a downward trend from 2000 to 2009 and a slight upward trend from 2009 to 2018. In brief, the vegetation coverage index declined significantly from 2000 to 2018, being 74.27 in 2000 but only 47.78 in 2018.

Table 5. Results of land use classification in Hetian.

Year	Forest Area (km²)	%	Grassland Area (km²)	%	Water Surfaces Area (km²)	%	Agriculture Area (km²)	%	Urban or Built-Up Area (km²)	%	Barren Land Area (km²)	%	Total Area km²	Biological Richness Index
1995	33,639.13	13.55%	9093.73	3.66%	13,585.53	5.47%	2555.60	1.03%	2456.92	0.99%	186,882.19	75.29%	248,213.10	40.65
2009	16,768.48	6.76%	30,349.04	12.23%	23,065.30	9.29%	3507.09	1.41%	6308.89	2.54%	168,218.42	67.77%	248,217.21	43.30
2018	16,877.60	6.85%	19,907.90	8.08%	21,798.60	8.84%	8036.65	3.26%	22,566.50	9.15%	157,339.00	63.82%	246,526.25	40.55

Table 6. Results of the vegetation coverage index in Hetian.

| Year	Extremely Low Area (km²)	%	Low Area (km²)	%	Moderate Area (km²)	%	High Area (km²)	%	Extremely High Area (km²)	%	Total Area km²	Vegetation Coverage Index
2000	63,312.90	25.68%	145,419.72	58.99%	17,965.65	7.29%	6845.36	2.78%	12,983.96	5.27%	246,527.59	74.27
2009	167,574.11	67.97%	59,158.23	24.00%	8828.43	3.58%	3938.83	1.60%	7028.09	2.85%	246,527.69	54.77
2018	193,514.84	78.50%	30,521.14	12.38%	9154.66	3.71%	5335.13	2.16%	8001.89	3.25%	246,527.65	47.78
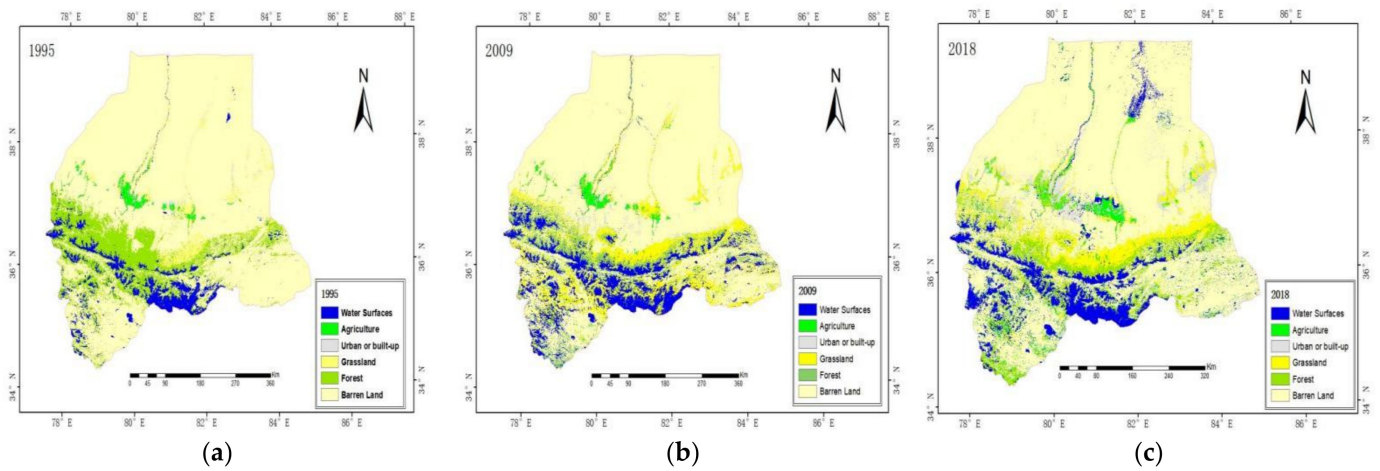
Figure 2. Results of land use classification in Hetian: (**a**) 1995; (**b**) 2009; (**c**) 2018.
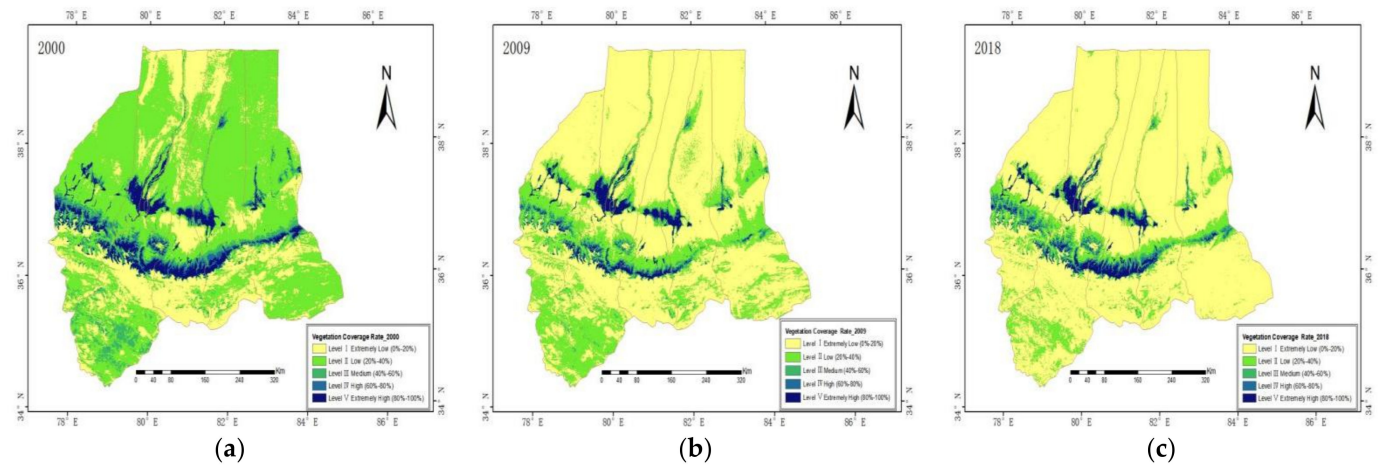

Figure 3. Results of vegetation coverage classification in Hetian: (**a**) 1995; (**b**) 2009; (**c**) 2018.

3.3. Water Network Denseness Index

After analyzing the water network denseness index in Hetian, we found that this index had values of 0.49, 0.52, and 0.52 in 1995, 2009, and 2018, respectively (Table 7). This index increased slightly over 25 years, but it remained below one.

Table 7. Results of the water network denseness index in Hetian.

Year	River Length (km)	Lake Area (km²)	Water Resources Quantity (km³)	Total Area (km²)	Water Network Denseness Index
1995	2648.35	228.14	7.32	246,527.00	0.49
2009	2648.35	272.00	7.64	246,527.00	0.52
2018	2648.35	269.04	11.01	246,527.00	0.52

3.4. Land Stress Index

The main external force causing soil erosion in Hetian is wind, and the degree of susceptibility to erosion depends on the slope, vegetation coverage, and land use type. From 1995 to 2018, the degree of change in areas of slight and mild soil erosion in Hetian was very small; however, the area of moderate erosion decreased significantly, from 61.15% to 19.36%, and areas of strong and severe erosion both increased (Figure 4). The land stress index is determined by severe soil erosion area, strong soil erosion area, urban or

built-up land area and other soil erosion area. The area of strong erosion changed from 58,779 to 143,798 km^2, but the area of other soil erosion declined from 178,735 to 64,877 km^2. In addition, the severe soil erosion area, which accounted for the largest weight in the calculation, did not change that significantly. Overall, although the soil erosion area has undergone major changes, the land stress index in Hetian has not changed significantly in the past 25 years, and its value has been stable at ~49 (Table 8).
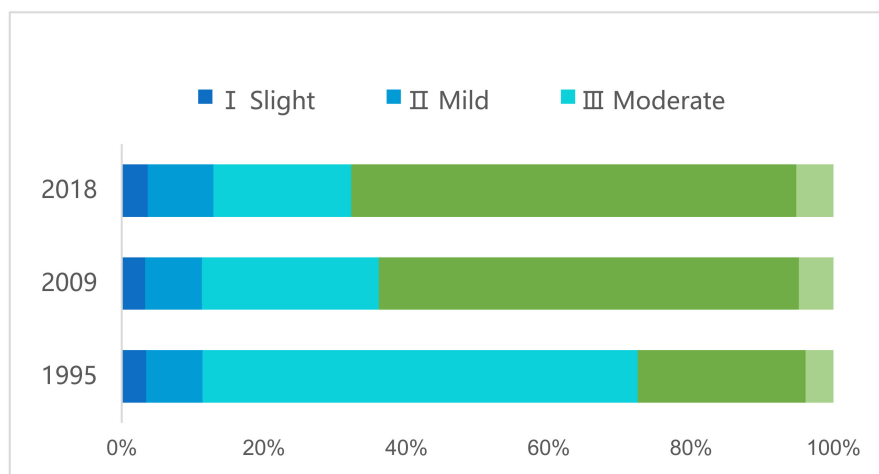

Figure 4. The area ratio of different soil erosion degrees in Hetian.

Table 8. Results of the land stress index in Hetian.

Year	Severe Soil Erosion Area (km^2)	Strong Soil Erosion Area (km^2)	Urban or Built-Up Land Area (km^2)	Other Soil Erosion Area (km^2)	Total Area (km^2)	Land Stress Index
1995	9767.59	58,779.60	2483.25	178,735.29	249,765.73	49.05
2009	11,456.07	143,798.12	6270.45	84,807.11	246,331.75	49.40
2018	11,288.79	147,621.79	22,543.83	64,877.26	246,331.67	49.37

3.5. Pollution Load Index

Generally, environmental pollution increases with the development of a city. Over the 25-year period in Hetian, the emissions of COD, ammoniacal nitrogen, sulfur dioxide, smoke, dust, and nitrogen oxide all increased significantly (Table 9), especially the emissions of COD, which showed a 3.5-fold increase from 1995 to 2018. However, the treatment and utilization of solid waste in Hetian has been conducted very well in recent years; it can be seen from the table below that the general solid waste discarded in Hetian in 2009 was 4900 tons—this decreased to only 2163 tons in 2018. According to the Hetian Yearbook in 2018, although the amount of general industrial solid waste generated in Hetian was 216,339 tons, the total utilization rate had reached 99%, making the amount of discarded solid waste very low, which indicates that Hetian had achieved remarkable success in the treatment of solid waste.

Table 9. Results of the pollution load index in Hetian.

Year	1995	2009	2018
COD Emissions (Ton)	2346.12	5151.22	8024.32
Ammonia Nitrogen Emissions (Ton)	389.14	832.91	1094.41
Sulfur Dioxide (Ton)	1437.00	5817.00	4335.00
Smoke and Dust Emissions (Ton)	2465.00	3440.00	3252.85
Nitrogen Oxides Emissions (Ton)	346.43	652.32	778.69
Solid Waste Emissions (Ton)	2516.00	4900.00	2163.00
Annual Precipitation (mm)	519.00	500.40	579.50
Total Area (km^2)	246,527.00	246,527.00	246,527.00
Pollution Load Index	10.00	22.42	27.34

*3.6. Grading and Changes of Eco-Environmental Status*

The EI has five sub-indices: biological richness, vegetation coverage, water network denseness, land stress, and pollution load. The first three indices are positively correlated with the eco-environment index, while the last two are negatively correlated. According to Tables 10 and 11 and Figure 5, the EI of Hetian in 1995 was 24.76, and the eco-environment status was relatively poor. With time, the EI of Hetian continued to decline, reaching 19.52 by 2009, with the eco-environment status dropping to poor. By 2018, the EI in Hetian was only 16.32; this indicates that the quality of the eco-environment in Hetian had declined significantly during the studied period.

Table 10. Results of EI in Hetian.

Year	Biological Richness Index	Vegetation Coverage Index	Water Network Denseness Index	Land Stress Index	Pollution Load Index	Ecological Index
1995	40.65	74.27	0.52	49.05	10.00	24.76
2009	43.30	54.77	0.52	49.40	22.42	19.52
2018	40.55	47.78	0.49	49.37	27.34	16.32

Table 11. Results of changes in the eco-environment in Hetian.

Periods	ΔEI	Level
1995–2009	−5.24	Obvious Change
2009–2018	−3.20	Obvious Change
1995–2018	−8.44	Significant Change
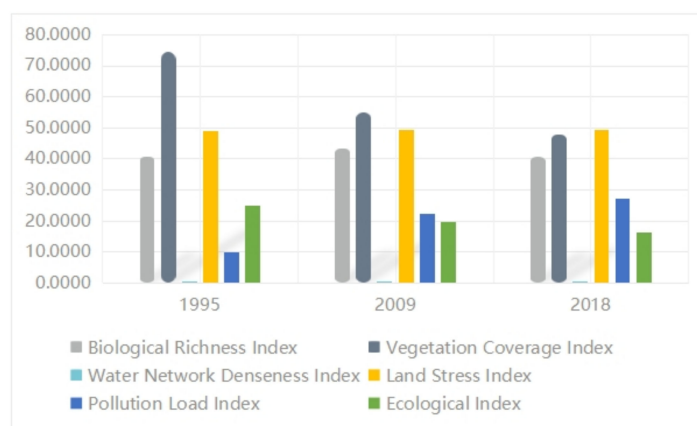
Figure 5. Changes in the eco-environment evaluation index in Hetian.

In addition, in the 15-year period from 1995 to 2009 and the 10-year period from 2009 to 2018, the value of the change in index ΔEI was in the range of $-3 \geq \Delta\text{EI} > -8$,

indicating that, in these two periods, the eco-environment quality in Hetian had deteriorated significantly. Furthermore, the EI showed large fluctuations, thus indicating that the eco-environment in Hetian was very sensitive.

4. Discussion

4.1. The Reduction in Vegetation Coverage and Reforestation

The vegetation coverage rate declined sharply from 1995 to 2018 in Hetian, by which the vegetation coverage index decreased from 74.26 to 47.78. This index is positively correlated with EI and has a considerable weight (25%) in the calculation of EI. Therefore, the substantial decline in the vegetation coverage in the Hetian area significantly affected the overall eco-environment quality. The reduction of vegetation coverage happened not only Hetian but also other arid or hyper-arid land such as Shiyang River Basin, Manas River Basin and Yili River Basin, and these areas are all located in arid region of Northwest China [43–45]. Agricultural encroachment is a possible reason that caused the reduction of vegetation [46]. Many places in arid land have great potential for agricultural development. Due to the location and climate, they have a long duration of sunshine, sufficient heat, a significant temperature difference between day and night, and little precipitation [47,48]. This environment is very suitable for the development of arid agriculture, such as the cultivation of cotton, walnuts, and dates, which has prompted a great number of people to rely on the business of working on farms in Hetian. However, some illegal agricultural encroachments have led to a reduction in natural forests, forcing local government to initiate measures to moderate the spread of encroachment and to reassert authority over its forest resources [49]. Apart from this, deforestation is also a reason that leads to vegetation reduction. This may be due to the ecological transformation in China in the 1990s, when state-owned forest farms were developmentally stagnant, administrative institutions in many remote areas were unstable, and illegal logging was prevalent, resulting in a sharp decline in forest [50–52]. With the reform of the system and standardization of management, over-exploitative behaviors have significantly curtailed, and the recent reforestation efforts have had a positive effect on the increase in vegetation coverage. However, forests also affect the water and soil resources on which they depend. For example, afforestation greatly increases the use of water resources, and it may pose potential risks of salinizing and acidifying the surrounding soil [53]. Therefore, it is necessary for the Government to balance the interaction between afforestation and water and soil conservation.

4.2. The Drivers of Land Use Changes and the Desertification of Hyper-Arid Areas

Although the overall habitat quality index in Hetian did not change significantly from 1995 to 2018, the land use varied with time. For instance, the forest area decreased to 16,878 km^2 in 2018, having had a value of 33,639 km^2 in 1995; the agricultural land increased three times in 2018 compared to its area in 1995, from 2557 to 8037 km^2; and the urban or built-up area expanded sharply and reached a peak in 2018. The expansion of agricultural and constructional land was a common trend at a national scale. Comparing to some other arid regions of Tarim Basin, the social and economic development of Hetian was profound [54,55]. However, the increase in population has led to a high demand for resources and living space, which has resulted in land use changes, such as the expansion of construction land and the reduction in forest [56]. Agriculture—the most important industry in Hetian—has always brought the greatest economic revenue to locals. The development of agriculture also impacts the land use change, such the growth of the agricultural area. Additionally, natural factors are possible reasons for the land use change. For example, global warming causes higher evaporation, which may lead to a reduction in surface runoff. In addition, the results of this study also provide evidence of the desertification of the hyper-arid land. Although the current UNCCD definition of desertification to include hyper-arid areas has recently been questioned [57], the results of this study demonstrate degradation in a hyper-arid region. EI is an indicator to identify the changes in an eco-environment. In Hetian, the EI declined from 24.76 to 16.32 in the

studied period, and this decline indicates degradation, which means that desertification could happen in the hyper-arid region.

4.3. The Pollution Load and the Necessary of Pollution Control

Over 25 years in Hetian, the emissions of chemical oxygen demand (COD), ammoniacal nitrogen, sulfur dioxide, smoke, dust, and nitrogen oxides have all increased significantly. COD is an important indicator of organic pollution in water. Ammoniacal nitrogen is a nutrient in water and can lead to water eutrophication; it is the main oxygen-consuming pollutant in the water and is poisonous to fish and some other aquatic organisms [58]. The increase in emissions of these two substances indicated that water pollution in Hetian has become increasingly serious in the past 25 years. The main industry in Hetian is agriculture, and water for agriculture also accounts for more than 90% of all water usage. Pesticides, chemical fertilizers, agricultural films remaining on farmland, improper disposal of agricultural livestock and poultry manure, malodorous gases, and unscientific aquaculture all produce water pollutants [59]; therefore, it is necessary to regulate the pollution caused to water bodies by agricultural production. Sulfur dioxide, smoke, dust, and nitrogen oxides are atmospheric pollutants; since 1995, with the aggravation of human activities in Hetian, the expansion of construction land, and the development of industry, air pollutants have inevitably increased, and air pollution will only have a negative impact upon the eco-environment. Therefore, pollution control is also very important for sustainable development of Hetian.

4.4. Applicability and Limitations of EI

This research selected EI as the eco-environment evaluation model. The EI is a comprehensive index that contains five sub-indices, and those sub-indices are factors affecting the eco-environment. The EI has good applicability in arid (or hyper-arid) areas because the research results are consistent with the observed data. Previous research that adopted the EI in the Tekes watershed, Ebinur Lake Basin, and Manas River Basin also demonstrated the applicability of the EI in drylands. The results of EI and its sub-indices can be used to reveal environmental issues in study areas and also have policy implications. Application of the EI requires sufficient remote sensing and statistical data because its sub-indices refer to various aspects. If more environment-related variables are added in EI, the results are more reliable. This is why preliminary investigations and surveys of research areas are necessary. Thus, a limitation is that calculating EI requires more time than other indices do. For example, the indicators that RSEI relies on are greenness, humidity, dryness, and heat, which can be extracted from only remote sensing images. As for EI, data are required not only from remote sensing images but also from statistics and surveys. Therefore, the EI needs more data support and research time compared with RSEI. In addition, the variables and weights of EI are relatively subjective, and the EI may ignore relevant information that affects the eco-environment. Moreover, some sub-indices such as pollution load index and water network denseness index are calculated using statistical data, and those data such as water resources quantity do not have coordinated information. Thus, the results of EI are hard to visualize in a map. Furthermore, there were a difference between the total land area of each studied years when calculated the biological richness index. Because the images from different sensors were used in the three studied years, inconsistency in spatial resolution or the size of raster cells of the generated thematic layer may result in inconsistency in the final statistical results.

5. Conclusions

This paper evaluated changes in the eco-environment quality of Hetian from 1995 to 2018 by using EI, which contains five sub-indices: the biological richness index, vegetation coverage index, water network denseness index, land stress index, and pollution load index. The results showed that the eco-environment in Hetian degraded significantly over these 25 years and that the EI declined from 24.76 to 16.32. These results indicated

desertification in Hetian, which can be seen as evidence of the desertification of hyper-arid areas. As for the policy implications, the policy-makers of Hetian should pay more attention to the continuous management and protection of the eco-environment and implement more protective measures, such as reducing pollutant emissions, adopting comprehensive measures to control water resources, strengthening measures to conserve water and soil resources, and increasing publicity and education on environmental protection. Ultimately, the eco-environment in Hetian could be sustainably developed and improved.

Author Contributions: Conceptualization, L.S.; methodology, L.S.; software, L.S. and X.Y.; validation, Y.Y. and R.Y.; investigation, Y.G. and J.H.; resources, L.S. and R.Y.; writing—original draft preparation, L.S.; writing—review and editing, L.S.; visualization, X.Y.; supervision, Y.Y., R.Y., I.M., and M.W.; project administration, R.Y.; funding acquisition, Y.Y. All authors have read and agreed to the published version of the manuscript.

Institutional Review Board Statement: Not applicable.

Informed Consent Statement: Not applicable.

Data Availability Statement: Not applicable.

References

1. Zheng, J.; Na, L.; Liu, B.; Zhang, T.; Wang, H. An Ecological Service System Based Study on Suburban Rural Landscape Multifunction. *Land* **2021**, *10*, 232. [CrossRef]
2. Shan, W.; Jin, X.; Ren, J.; Wang, Y.; Xu, Z.; Fan, Y. Ecological environment quality assessment based on remote sensing data for land consolidation. *J. Clean. Prod.* **2019**, *239*, 118–126. [CrossRef]
3. Snella, M.A.; Irvine, K.A. Importance of scalar and riparian habitat effects for assessment of ecological status using littoral diatoms. *Ecol. Indic.* **2013**, *25*, 149–155. [CrossRef]
4. Handfield, R.; Walton, S.V.; Sroufe, R.; Melnyk, S.A. Applying environmental criteria to supplier assessment: A study in the application of the Analytical Hierarchy Process. *Eur. J. Oper. Res.* **2002**, *141*, 70–87. [CrossRef]
5. Delfanti, L.; Colanton, A.; Zambon, I.; Salvat, L. Solar plants, environmental degradation and local socioeconomic contexts: A case study in a Mediterranean country. *Environ. Impact Assess. Rev.* **2016**, *61*, 88–93. [CrossRef]
6. Wang, Q.; Li, W.; Li, T.; Li, X.; Liu, S. Goafwater storage and utilization in arid regions of northwest China: A case study of Shennan coal mine district. *J. Clean. Prod.* **2018**, *202*, 33–44. [CrossRef]
7. Yu, X.; Hawley-Howard, J.; Pitt, A.L.; Wang, J.-J.; Baldwin, R.F.; Chow, A.T. Water quality of small seasonal wetlands in the Piedmont ecoregion, South Carolina, USA: Effects of land use and hydrological connectivity. *Sci. Direct* **2015**, *73*, 98–108. [CrossRef]
8. Yang, Z.; Li, W.; Li, X.; Wang, Q.; He, J. Assessment of eco-geo-environment quality using multivariate data: A case study in a coal mining area of Western China. *Ecol. Indic.* **2019**, *107*, 105651. [CrossRef]
9. Pandey, S.K.; Bhattacharya, T. Mobility, Ecological risk and change in surface morphology during sequential chemical extraction of heavy metals in fly ash: A case study. *Environ. Technol. Innov.* **2019**, *13*, 373–382. [CrossRef]
10. Popp, J.H.; Hyatt, D.E.; Hoag, D. Modeling environmental condition with indices: A case study of sustainability and soil resources. *Ecol. Model.* **2000**, *30*, 131–143. [CrossRef]
11. Shi, L.; Yang, S. Assessment of Eco-Environmental Stress in the Western Taiwan Straits Economic Zone. *Sustainability* **2015**, *7*, 2716–2729. [CrossRef]
12. Zhao, W.; Yan, T.; Ding, X.; Peng, S.; Chen, H.; Fu, Y. Response of ecological quality to the evolution of land use structure in Taiyuan during 2003 to 2018. *Alex. Eng. J.* **2021**, *60*, 1777–1785. [CrossRef]
13. Feng, D.; Bao, W.; Fu, M.; Zhang, M.; Sun, Y. Current and Future Land Use Characters of a National Central City in Eco-Fragile Region—A Case Study in Xi'an City Based on FLUS Model. *Land* **2021**, *10*, 286. [CrossRef]
14. Xu, F.; Zhou, J.; Li, B.; Cao, J.; Tao, S. Multi -step Fuzzy Cluster Analysis for Comprehensive Assessment of Urban Environmental Quality. *Urban Environ. Urban Ecol.* **2001**, *14*, 13–15. (In Chinese)
15. Yu, L.; Yi, W. Application Research of Analytic Hierarchy Process (AHP) in Urban Ecotope Quality Evaluation. *Sichuan Environ.* **2002**, *21*, 38–40. (In Chinese) [CrossRef]
16. Hao, Y.; Zhou, H. A Grey Assessment Model of Regional Eco-evironment Quality and Its Application. *Environ. Eng.* **2002**, *20*, 66–70. (In Chinese) [CrossRef]
17. Tang, L.; Zhang, L.; Wang, Z. Application of Artificial Neural Network to the Assessment of Eco-environment Quality. *Sichuan Environ.* **2003**, *22*, 69–72. (In Chinese) [CrossRef]

18. Xu, Y.; Zhou, H. A Preliminary Study on Advances in Assessment of Eco-environmental Quality in China. *Arid Land Geogr.* **2003**, *26*, 166–172. [CrossRef]

19. Xu, H. A remote sensing urban ecological index and its application. *Acta Ecol. Sin.* **2013**, *33*, 7853–7862. (In Chinese) [CrossRef]

20. Xu, H. A remote sensing index for assessment of regional ecological changes. *China Environ. Sci.* **2013**, *33*, 889–897. (In Chinese)

21. China MoEaEotPsRo. Technical Criterion for Ecosystem Status Evaluation. 2015; p. 28. (In Chinese). Available online: http://english.mee.gov.cn/Resources/standards/Eco_Environment/201605/t20160512_337614.shtml (accessed on 10 October 2020).

22. Zhang, Z. Eco-Environmental Monitoring and Evaluation of Tekes Watershed in Xinjiang Using Remote Sensing Images. Master's Thesis, China University of Geosciences, Beijing, China, 2012. Available online: http://kns.cnki.net/kcms/detail/detail.aspx?DBCode=CMFD&DBName=CMFD201301&fileName=1012365210.nh (accessed on 1 February 2021).

23. Lin, M. Evaluation of Ecological Environment Quality in Danjiangkou Water Source Area Based on RS and GIS in Hubei Province. Master's Thesis, Hubei University, Wuhan, China, 2019. [CrossRef]

24. Gong, Z.; Li, M. Research on the Method of Assessment of Natural Ecology for Tibet Plateau Ecological Shelter Zone. *Geomat. Spat. Inf. Technol.* **2020**, *43*, 88–92, 95. Available online: http://kns.cnki.net/kcms/detail/detail.aspx?DBCode=CJFD&DBName=CJFDLAST2020&fileName=DBCH202011025 (accessed on 1 February 2021).

25. Kasim, Y. Spatial-Temporal Differentiation and Influence Factors of Economic-Ecosystem Coupling in Ebinur Lake. Ph.D. Thesis, Xinjiang University, Urumqi, China, 2019. Available online: http://kns.cnki.net/kcms/detail/detail.aspx?DBCode=CJFD&DBName=CJFDLAST2020&fileName=DBCH202011025//kns.cnki.net/kcms/detail/detail.aspx?DBCode=CDFD&DBName=CDFDLAST2019&fileName=1019608487.nh (accessed on 25 September 2020).

26. Liu, H.; Liu, Z. Analysis on the Status and Variations of Ecological Environment in the Pearl River Delta Urban Agglomeration from 2011 to 2015. *China Resour. Compr. Util.* **2019**, *37*. [CrossRef]

27. Ouyang, L.; Ma, H.; Wang, Z.; Wang, Z.; Yu, X. Assessment of ecological environment in Chifeng City based on Landsat imagery. *China Environ. Sci.* **2020**, *40*, 5075. [CrossRef]

28. Chen, L. Study on the Ecological Environment of Manas River Basin Shihezi. Master's Thesis, Shihezi University, Shihezi, China, 2020. [CrossRef]

29. He, K.; Wu, S.; Yang, Y.; Wang, D.; Zhang, S.; Yin, N. Dynamic changes of land use and oasis in Xinjiang in the last 40 years. *Arid Land Geogr.* **2018**, *46*, 1333–1340. (In Chinese) [CrossRef]

30. Sun, Z.; Chang, N.-B.; Oppc, C.; Hennig, T. Spatial and temporal characteristics of aridity conditions in Tarim Basin, China. *Earth Resour. Environ. Remote Sens. GIS Appl.* **2010**, *7831*, 78311R. [CrossRef]

31. Tan, R. Research on the Pattern and Path of Industrala Poverty Alleviation in Hetian, Xinjiang. Master's Thesis, Tianjing Normal University, Tianjing, China, 2020. (In Chinese) [CrossRef]

32. Wang, Q.; Ma, Z.; Ma, Q.; Liu, M.; Yuan, X.; Mu, R.; Zuo, J.; Zhang, J.; Wang, S. Comprehensive evaluation and optimization of agricultural system: An emergy approach. *Ecol. Indic.* **2019**, *107*, 105650. [CrossRef]

33. Kosmas, C.; Kirkby, M.J.; Geeson, N. (Eds.) *EC-European Commission The Medalus Project: Mediterranean Desertification and Land Use: Manual on Key Indicators of Desertification and Mapping Environmentally Sensitive Areas to Desertification*; Directorate-General Science, Research and Development: Paris, France, 1999.

34. Yuan, Y.; Na, Z.; Yongdong, W. Comparative study of desertification control policies and regulations in representative countries of the Belt and Road Initiative. *Glob. Ecol. Conserv.* **2021**, *27*, e01577. [CrossRef]

35. Wang, T. Review and Prospect of Research on Oasification and Desertification in Arid Regions. *Acta Geogr. Sin.* **2004**, *29*, 1–9. Available online: http://kns.cnki.net/kcms/detail/detail.aspx?DBCode=CJFD&DBName=CJFDLAST2020&fileName=DBCH202011025//kns.cnki.net/kcms/detail/detail.aspx?DBCode=CJFD&DBName=CJFD2004&fileName=DLXB200402006 (accessed on 20 May 2021).

36. Chen, X.; Chang, C.; Bao, A.; Wu, S.; Luo, G. Spatial pattern and characteristics of land cover change in Xinjiang since past 40 years of the economic reform and opening up. *Arid Land Geogr.* **2020**, *43*, 1–11. (In Chinese) [CrossRef]

37. Dias, V.; Belcher, K. Value and provision of ecosystem services from prairie wetlands: A choice experiment approach. *Ecosyst. Serv.* **2015**, *15*, 35–44. [CrossRef]

38. Serra, P.; Vera, A.; Tulla, A.F.; Salvati, L. Beyond urbanerural dichotomy: Exploring socioeconomic and land-use processes of change in Spain (1991–2011). *Appl. Geogr.* **2014**, *55*, 71–81. [CrossRef]

39. Britannica. Available online: https://www.britannica.com/science/habitat-biology (accessed on 13 August 2021).

40. Hughes, R.M.; Herlihy, A.T.; Kaufmann, P.R. An Evaluation of Qualitative Indexes of Physical Habitat Applied to Agricultural Streams in Ten, U.S. States. *J. Am. Water Resour. Assoc.* **2010**, *46*, 792–806. [CrossRef]

41. Yang, Y. Evolution of habitat quality and association with land-use changes in mountainous areas: A case study of the Taihang Mountains in Hebei Province, China. *Ecol. Indic.* **2021**, *129*, 107967. [CrossRef]

42. Angulo, E. The Tomlinson Pollution Load Index applied to heavy metal, 'Mussel-Watch' data: A useful index to assess coastal pollution. *Sci. Total Environ.* **1996**, *187*, 19–56. [CrossRef]

43. Chang, J. Evaluation of Eco-Environmental Quality in Arid Region Based on Spatio-Temporal Dynamics: A Case Study of Shiyang River Basin in Gansu Province. Ph.D. Thesis, Shanxi Narmal University, Xi'an, China, 2011.

44. Wang, J.; Ma, J.; Xie, F.; Xu, X. Improvement of remote sensing ecological index in arid regions: Taking Ulan Buh Desert as an example. *Chin. J. Appl. Ecol.* **2020**, *31*, 3795–3804. [CrossRef]

45. Wang, H.; Zhang, X.; Qiao, M.; Miu, Y. Evaluation and dynamic analysis of ecological environment quality in Yili River Basin based on GIS. *Arid Land Geogr.* **2008**, *31*. [CrossRef]
46. Ding, Y.; Abdirahman, H.; Chen, X.; Mukaddas, A. Spatial-temporal changes in vegetation characteristics and climate in Hotan Prefecture. *Acta Ecol. Sin.* **2020**, *40*, 1258–1268. [CrossRef]
47. Peng, J.; Liu, T.; Huang, Y.; Ling, Y.; Li, Z.; Bao, A.; Chen, X.; Kurban, A.; De Maeyer, P. Satellite-Based Precipitation Datasets Evaluation Using Gauge Observation and Hydrological Modeling in a Typical Arid Land Watershed of Central Asia. *Remote Sens.* **2021**, *13*, 221. [CrossRef]
48. Wang, H.; He, M.; Yan, W.; Ai, J.; Chu, J. Ecosystem vulnerability in the Tianshan Mountains and Tarim Oasis based on remote sensed gross primary productivity. *Acta Ecol. Sin.* **2021**, *41*, 24. Available online: https://kns.cnki.net/kcms/detail/11.2031.Q.20210803.1506.054.html (accessed on 20 May 2021).
49. Gao, F.; Deng, F. Preliminary study on the transfer of factors of agricultural production in xinjiang. *J. Xinjiang Univ.* **1993**, *3*, 51–55. Available online: https://kns.cnki.net/kcms/detail/detail.aspx?dbcode=CJFD&filename=XJDZ199303008&dbname=CJFD9093 (accessed on 1 February 2021).
50. Sun, S.; Wang, L.; Che, K. Analysis of Vegetation Coverage Change in Diebu Forest of the Upper Bailong River Base on Landsat Satellite Data. *J. Sichuan Agric. Univ.* **2016**, *34*, 39–41. (In Chinese)
51. Jie, W.; Dongwei, L.; Jiali, M.; Yingnan, C.; Lixin, W. Development of a large-scale remote sensing ecological index in arid areas and its application in the Aral Sea Basin. *J. Arid Land* **2021**, *13*, 40–55. [CrossRef]
52. Daniela, S.; Tomaso, C.; Sofia, B.; Luca, S.; Luigi, P. Linking trajectories of land change, land degradation processes and ecosystem services. *Environ. Res.* **2016**, *147*, 590–600. [CrossRef]
53. Kordrostami, F.; Attarod, P.; Abbaspour, K.C.; Ludwig, R.; Etemad, V.; Alilou, H.; Bozorg-Haddad, O. Identification of optimum afforestation areas considering sustainable management of natural resources, using geo-environmental criteria. *Ecol. Eng.* **2021**, *168*, 106259. [CrossRef]
54. Liu, M.; Jiang, Y.; Xu, X.; Huang, Q.; Huo, Z.; Huang, G. Long-term groundwater dynamics affected by intense agricultural activities in oasis areas of arid inland river basins, Northwest China. *Agric. Water Manag.* **2018**, *203*, 37–52. [CrossRef]
55. Duarte, B.; Goessling, J.W.; Marques, J.C.; Caçador, I. Ecophysiological constraints of Aster tripolium under extreme thermal events impacts: Merging biophysical, biochemical and genetic insights. *Plant Physiol. Biochem.* **2015**, *97*, 217–228. [CrossRef]
56. Silleos, N.G.; Alexandridis, T.K.; Gitas, I.Z.; Perakis, K. Vegetation Indices: Advances Made in Biomass Estimation and Vegetation Monitoring in the Last 30 Years. *Geocarto Int.* **2008**, *21*, 21–28. [CrossRef]
57. Martínez-Valderrama, J.; Guirado, E.; Maestre, F.T. Desertifying deserts. *Nat. Sustain* **2020**, *3*, 572–575. [CrossRef]
58. Briner, S.; Elkin, C.; Huber, R. Evaluating the relative impact of climate and economic changes on forest and agricultural ecosystem services in mountain regions. *J. Environ. Manag.* **2013**, *129*, 414–422. [CrossRef]
59. Liu, Y. Combined Utilization Research of Surface Water and Groundwater in Oasis Irrigation District of Southern Margin of Tarim Basin—A Case Study of Cele Oasis. Master's Thesis, Xinjiang Unversity, Urumqi, China, 2019. Available online: https://kns.cnki.net/kcms/detail/detail.aspx?dbcode=CDFD&dbname=CDFDLAST2019&filename=1019608491.nh&v=9Vj%25mmd2BSkieQH4SL%25mmd2FpBzrvC6xpWG8rrdFxdS6NsiAIST6wcAriVH%25mmd2FIxzUpieliHOw0T (accessed on 1 February 2021).